

When Extrasolar Planets Transit Their Parent Stars

David Charbonneau

Harvard-Smithsonian Center for Astrophysics

Timothy M. Brown

High Altitude Observatory

Adam Burrows

University of Arizona

Greg Laughlin

University of California, Santa Cruz

When extrasolar planets are observed to transit their parent stars, we are granted unprecedented access to their physical properties. It is only for transiting planets that we are permitted direct estimates of the planetary masses and radii, which provide the fundamental constraints on models of their physical structure. In particular, precise determination of the radius may indicate the presence (or absence) of a core of solid material, which in turn would speak to the canonical formation model of gas accretion onto a core of ice and rock embedded in a protoplanetary disk. Furthermore, the radii of planets in close proximity to their stars are affected by tidal effects and the intense stellar radiation. As a result, some of these “hot Jupiters” are significantly larger than Jupiter in radius. Precision follow-up studies of such objects (notably with the space-based platforms of the *Hubble* and *Spitzer Space Telescopes*) have enabled direct observation of their transmission spectra and emitted radiation. These data provide the first observational constraints on atmospheric models of these extrasolar gas giants, and permit a direct comparison with the gas giants of the Solar system. Despite significant observational challenges, numerous transit surveys and quick-look radial velocity surveys are active, and promise to deliver an ever-increasing number of these precious objects. The detection of transits of short-period Neptune-sized objects, whose existence was recently uncovered by the radial-velocity surveys, is eagerly anticipated. Ultra-precise photometry enabled by upcoming space missions offers the prospect of the first detection of an extrasolar Earth-like planet in the habitable zone of its parent star, just in time for Protostars and Planets VI.

1. OVERVIEW

The month of October 2005, in which the fifth Protostars and Planets meeting was held, marked two important events in the brief history of the observational study of planets orbiting nearby, Sun-like stars. First, it was the ten-year anniversary of the discovery of 51 Pegb (*Mayor and Queloz*, 1995), whose small orbital separation implied that similar hot Jupiters could be found in orbits nearly co-planar to our line of sight, resulting in mutual eclipses of the planet and star. Second, October 2005 heralded the discovery of the ninth such transiting planet (*Bouchy et al.*, 2005a). This select group of extrasolar planets has enormous influence on our overall understanding of these objects: The 9 transiting planets are the only ones for which we have accurate estimates of key physical parameters such as mass, radius, and, by inference, composition. Furthermore, precise monitoring of these systems during primary and secondary eclipse has permitted the direct study of their atmospheres. As a result, transiting planets are the only ones whose physical

structure and atmospheres may be compared in detail to the planets of the Solar system, and indeed October 2005 was notable for being the month in which the number of objects in the former category surpassed the latter.

Our review of this rapidly-evolving field of study proceeds as follows. In Section 2, we consider the physical structure of these objects, beginning with a summary of the observations (Section 2.1) before turning to their impact on our theoretical understanding (Section 2.2). In Section 3, we consider the atmospheres of these planets, by first summarizing the challenges to modeling such systems (Section 3.1), and subsequently reviewing the detections and upper limits, and the inferences they permit (Section 3.2). We end by considering the future prospects (Section 4) for learning about rocky planets beyond the Solar system through the detection and characterization of such objects in transiting configurations.

2. PHYSICAL STRUCTURE

2.1. Observations

2.1.1. Introduction. When a planet transits, we can accurately measure the orbital inclination, i , allowing us to evaluate the planetary mass M_{pl} directly from the minimum mass value $M_{pl} \sin i$ determined from radial-velocity observations and an estimate of the stellar mass, M_* . The planetary radius, R_{pl} , can be obtained by measuring the fraction of the parent star's light that is occulted, provided a reasonable estimate of the stellar radius, R_* , is available. With the mass and radius in hand, we can estimate such critically interesting quantities as the average density and surface gravity. Hence, the information gleaned from the transiting planets allows us to attempt to unravel the structure and composition of the larger class of extrasolar planets, to understand formation and evolution processes (including orbital evolution), and to elucidate physical processes that may be important in planetary systems generically. Fig. 1 shows the mass-radius relation for the 9 known transiting planets, with Jupiter and Saturn added for comparison. It is fortunate that the present small sample of objects spans a moderate range in mass and radius, and appears to contain both a preponderance of planets whose structure is fairly well described by theory, as well as a few oddities that challenge our present knowledge.

We begin by describing how the objects shown in Fig. 1 were identified and characterized, and, along the way, we illuminate the limitations that these methods imply for our efforts to understand extrasolar planets as a class. By definition, transiting planets have their orbits oriented so that the Earth lies nearly in their orbital plane. This is an uncommon occurrence; assuming random orientation of planetary orbits, the probability that a planet with orbital eccentricity, e , and longitude of periastron, ϖ , produces transits visible from the Earth is given by

$$P_{tr} = 0.0045 \left(\frac{1 \text{ AU}}{a} \right) \left(\frac{R_* + R_{pl}}{R_\odot} \right) \left[\frac{1 + e \cos(\frac{\pi}{2} - \varpi)}{1 - e^2} \right]$$

which is inversely proportion to a , the orbital semi-major axis. All known transiting planets have orbital eccentricities consistent with zero, for which the last factor in the above equation reduces to unity.

The radii of Jovian planets are typically only about 10% of the stellar radii. The transits known to date result in a 0.3 – 3% diminution of the stellar flux reaching the Earth. These transits last for 1.5 – 3.5 hours, and accurate ground-based characterizations of these events are challenging. The paucity and subtlety of the transits make it necessary to use great care to reduce the random errors and systematic biases that plague the estimation of the planets' fundamental properties (Section 2.1.4).

2.1.2. Methods of Detection. The presently-known transiting planets have all been detected by one of the two following means, both foreseen by *Struve* (1952): (1) Photometric detection of transit-like events, with subsequent con-

firmation of planetary status via radial-velocity measurements, and (2) radial-velocity detection of a planet with subsequent measurement of photometric transits. Radial velocity detection has the advantage that the planetary nature of the target object is generally unambiguous. Its disadvantage is that it requires substantial observing time on large telescopes to identify each planetary system, and only then can the relatively cheap process of searching for photometric transits begin. Direct photometric transit searches simultaneously monitor large numbers of stars in a given field of view, but suffer from a very high rate of astrophysical false positives (Section 2.1.3).

Successful photometric transit searches have so far adopted one of two basic strategies, using either moderate-sized or very small telescopes to search either fainter or brighter stars. Five transiting planets (OGLE-TR-10b, 56b, 111b, 113b, and 132b) have been detected by the Optical Gravitational Lensing Experiment (OGLE) survey (*Udalski et al.*, 2002a, 2002b, 2002c, 2003, 2004), which uses a 1.3 m telescope. The parent stars of these planets are faint (typically $V = 16.5$). The large-telescope follow-up observations needed to verify their planetary status, to measure the stellar reflex velocities, and to estimate the planetary masses and radii have been conducted by several groups (*Bouchy et al.*, 2004, 2005b; *Dreizler et al.*, 2002; *Konacki et al.*, 2003a, 2003b, 2004, 2005; *Moutou et al.*, 2004; *Pont et al.*, 2004; and *Torres et al.*, 2004a, 2004b, 2005).

The Trans-Atlantic Exoplanet Survey (TrES) employed a network of 3 automated small-aperture (10 cm), wide-field ($6^\circ \times 6^\circ$) telescopes (*Brown and Charbonneau*, 2000; *Dunham et al.*, 2004; *Alonso*, 2005) to detect the planet TrES-1 (*Alonso et al.*, 2004; *Sozzetti et al.*, 2004). Its parent star ($V = 11.8$) is significantly brighter than the OGLE systems, but fainter than the transiting-planet systems detected by radial-velocity surveys (below). Because of this relative accessibility, TrES-1 has also been the subject of intensive follow-up observations, as detailed later in this review.

Numerous other photometric transit surveys are active at the current time. The BEST (*Rauer et al.*, 2005), HAT (*Bakos et al.*, 2004), KELT (*Pepper et al.*, 2004), Super-WASP (*Christian et al.*, 2005), Vulcan (*Borucki et al.*, 2001), and XO (*McCullough et al.*, 2005) surveys, and the proposed PASS (*Deeg et al.*, 2004) survey all adopt the small-aperture, wide-field approach, whereas the EXPLORE (*Mallen-Ornelas et al.*, 2003) project employs larger telescopes to examine fainter stars. The benefits of surveying stellar clusters (*Janes*, 1996; *Pepper and Gaudi*, 2005) have motivated several surveys of such systems, including EXPLORE/OC (*von Braun et al.*, 2005), PISCES (*Mochejska et al.*, 2005, 2006), and STEPSS (*Burke et al.*, 2004; *Marshall et al.*, 2005). An early, stunning null result was the *HST* survey of 34,000 stars in the globular cluster 47 Tuc, which points to the interdependence of the formation and migration of hot Jupiters on the local conditions, namely crowding, metallicity, and initial proximity to O and B stars (*Gilliland et al.*, 2000).

Finally, three transiting planets were first discovered by

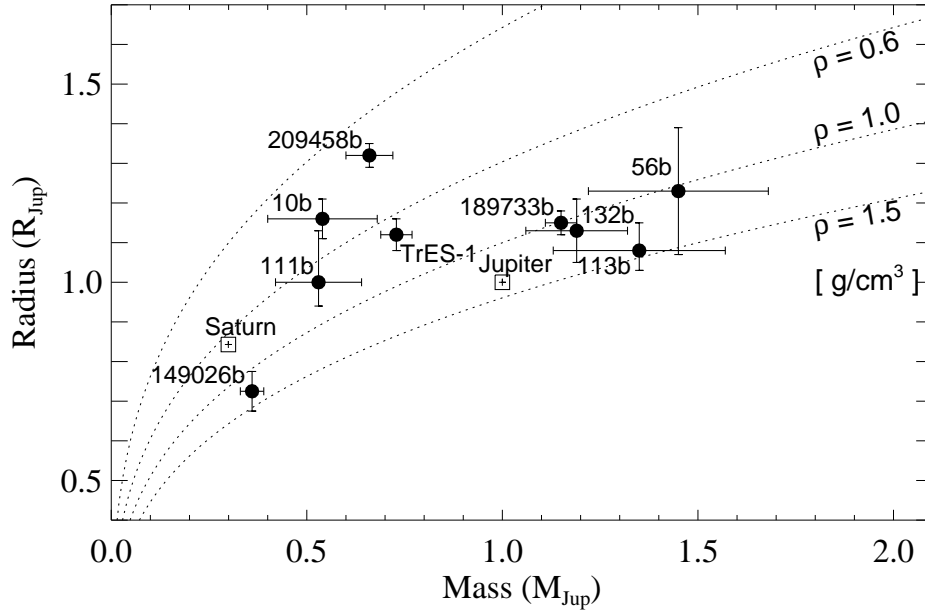


Fig. 1.— Masses and radii for the 9 transiting planets, as well as Jupiter and Saturn. The data are tabulated in Table 1, and are gathered from *Bakos et al., in preparation*, *Bouchy et al. (2004, 2005b)*, *Brown et al., in preparation*, *Charbonneau et al. (2006)*, *Holman et al. (2005)*, *Knutson et al. (2006)*, *Laughlin et al. (2005a)*, *Moutou et al. (2004)*, *Pont et al. (2004)*, *Sato et al. (2006)*, *Sozzetti et al. (2004)*, *Torres et al. (2004a)*, and *Winn et al. (2005)*.

radial-velocity surveys. These include HD 209458b, the first transiting planet discovered (*Charbonneau et al., 2000; Henry et al., 2000; Mazeh et al., 2001*), and the two most recently discovered transiting planets, HD 149026b (*Sato et al., 2005*) and HD 189733b (*Bouchy et al., 2005a*). The latter two objects were uncovered by quick-look radial-velocity surveys targeted at identifying short-period planets of metal-rich stars (respectively, the N2K Survey, *Fischer et al., 2005*; and the Elodie Metallicity-Biased Search, *da Silva et al., 2006*). Given the preference of radial-velocity surveys for bright stars, it is not surprising that all three systems are bright ($7.6 < V < 8.2$), making them natural targets for detailed follow-up observations. As we shall see below, HD 209458b has been extensively studied in this fashion. Similar attention has not yet been lavished on the other two, but only because of their very recent discovery.

2.1.3. Biases and False Alarms. Photometric transit surveys increase their odds of success by simultaneously observing as many stars as possible. Hence, their target starfields are moderately to extremely crowded, and the surveys must therefore work near the boundary of technical feasibility. The constraints imposed by the search method influence which kinds of planets are detected.

Photometric transit searches are strongly biased in favor of planets in small orbits, since such objects have a greater probability of presenting an eclipsing configuration (Section 2.1.1). Moreover, most transit searches require a minimum of 2 (and usually 3) distinct eclipses to be ob-

served, both to confirm the reality of the signal, and to permit an evaluation of the orbital period. Since larger orbits imply longer orbital periods and fewer chances for transits to occur, small orbits are preferred for transit surveys with only a limited baseline. This is frequently the regime in which single-site surveys operate. However, multi-site surveys that monitor a given field for several months (e.g. HAT, TrES) frequently achieve a visibility (the fraction of systems of a given period for which the desired number of eclipse events would be observed) nearing 100% for periods up to 6 days. As a result, such surveys do not suffer this particular bias, although admittedly only over a limited range of periods. Similarly, a stroboscopic effect can afflict single-site surveys, favoring orbital periods near integer numbers of days and may account for the tendency of the longer-period transiting planet periods to clump near 3 and 3.5 days (*Pont et al., 2004, Gaudi et al., 2005*). This situation occurs if the campaign is significantly shorter in duration than that required to achieve complete visibility across the desired range of orbital periods. However, for observing campaigns for which more than adequate phase coverage has been obtained, the opposite is true, and periods near integer and half-integer values are disfavored. The limiting example of this situation would be a single-site campaign consisting of thousands of hours of observations, which nonetheless would be insensitive to systems with integer periods, if their eclipses always occur when the field is below the horizon.

Most field surveys operate in a regime limited by the

signal-to-noise of their time series (which are typically searched by an algorithm than looks for statistically-significant, transit-like events, e.g. Kovács *et al.*, 2002), and for which the number of stars increases with decreasing flux (a volume effect). An important detection bias for surveys operating under such conditions has been discussed by Pepper *et al.* (2003) and described in detail by Gaudi *et al.* (2005), Gaudi (2005), and Pont *et al.* (2005). These surveys can more readily detect planets with shorter periods and larger radii orbiting fainter stars, and since such stars correspond to a large distance (hence volume) they are much more numerous. As a result, any such survey will reflect this bias, which cannot be corrected merely by improving the cadence, baseline, or precision of the time series (although improving the latter will reduce the threshold of the smallest planets that may be detected).

Most ongoing transit surveys are plagued by a high rate of candidate systems displaying light curves that precisely mimic the desired signal, yet are not due to planetary transits. We can divide such false positives into three broad categories: Some are true *statistical* false positives, resulting from selecting an overly-permissive detection threshold whereby the light-curve search algorithm flags events that result purely from photometric noise outliers (Jenkins *et al.*, 2002). The second source is *instrumental*, due to erroneous photometry, often resulting from leakage of signal between the photometric apertures of nearby stars in a crowded field. However, the dominant form, which we shall term *astrophysical* false positives, result from eclipses among members of double- or multiple-star systems. Grazing eclipses in binary systems can result in transit-like signals with depths and durations that resemble planetary ones (Brown, 2003), and this effect is especially pronounced for candidate transits having depths greater than 1%. (For equal-sized components, roughly 20% of eclipsing systems have eclipse depths that are less than 2% of the total light.) In these cases the eclipse shapes are dissimilar (grazing eclipses produce V-shapes, while planetary transits have flat bottoms), but in noisy data, this difference can be difficult to detect. A false alarm may also occur when a small star transits a large one (e.g., an M-dwarf eclipsing a main-sequence F star). Since the lowest-mass stars have Jupiter radii, it is not surprising that such systems mimic the desired signal closely: They produce flat-bottomed transits with the correct depths and durations. Larger stars eclipsing even larger primaries can also mimic the desired signal, but a careful analysis of the transit shape can often reveal the true nature of the system (Seager and Mallen-Ornelas, 2003). Other useful diagnostics emerge from careful analysis of the light curve outside of eclipses. These can reveal weak secondary eclipses, periodic variations due to tidal distortion or gravity darkening of the brighter component, or significant color effects. Any of these variations provides evidence that the eclipsing object has a stellar mass as opposed to a planetary mass (Drake, 2003; Sirko and Paczyński, 2003; Tingley, 2004). In the absence of these diagnostics, the stellar nature of most companions is easily revealed by low-precision (1 km s^{-1})

radial velocity measurements, since even the lowest-mass stellar companions cause reflex orbital motions of tens of km s^{-1} (for examples, see Latham, 2003; Charbonneau *et al.*, 2004; Bouchy *et al.*, 2005b; Pont *et al.*, 2005).

The most troublesome systems are hierarchical triple stars in which the brightest star produces the bulk of the system’s light, and the two fainter ones form an eclipsing binary. In such cases, the depths of the eclipses are diluted by light from the brightest member, and often radial velocity observations detect only the bright component as well. Given neither radial velocity nor photometric evidence for a binary star, such cases can easily be mistaken for transiting planets. Correct identification then hinges on more subtle characteristics of the spectrum or light curve, such as line profile shapes that vary with the orbital period (Mandushev *et al.*, 2005; Torres *et al.*, 2004b, 2005), or color dependence of the eclipse depth (O’Donovan *et al.*, 2006). Because of the large preponderance of false alarms over true planets, it is only after all of the above tests have been passed that it makes sense to carry out the resource-intensive high-precision radial-velocity observations that establish beyond question that the transiting object has a planetary mass.

2.1.4. Determining the Radii and Masses. After transiting planets are identified, an arsenal of observing tools is available (and necessary) for their characterization. An accurate estimate of M_{pl} requires precise radial-velocity measurements (from which the orbital elements P , e , and ϖ are also determined), as well as an estimate of M_* . The former are gathered with high-dispersion echelle spectrographs fed by large telescopes. For bright parent stars, precision of a few m s^{-1} (compared to reflex orbital speeds of $50 - 200 \text{ m s}^{-1}$) can be obtained with convenient exposure times, so that uncertainties in the velocity measurements do not dominate the estimate of M_{pl} . In this regime, the greatest source of uncertainty is the value of M_* itself. Given the difficulty of estimating the ages of field stars, comparison with grids of stellar models (e.g. Girardi *et al.*, 2002) suggests that mass estimates are likely to be in error by as much as 5%. This uncertainty could be removed by measuring the orbital speed of the planet directly. Several efforts have sought to recover the reflected-light spectrum of the planet in a series of high-resolution stellar spectra spanning key phases of the orbital period, but have achieved only upper limits (Charbonneau *et al.*, 1999; Collier Cameron *et al.*, 2002; Leigh *et al.*, 2003a, 2003b). (These results also serve to constrain the wavelength-dependent planetary albedo, a topic to which we shall return in Section 3.2.2.) For faint parent stars, the radial-velocity estimates become more expensive and problematic, and contribute significantly to the final error budget for M_{pl} . Interestingly, the most intractable uncertainty concerning masses of non-transiting planets, namely the value of $\sin i$, is exquisitely well-determined by fits to the transit light curve.

Analysis of moderate-precision light curves (obtained with ground-based telescopes) nonetheless yield a tight

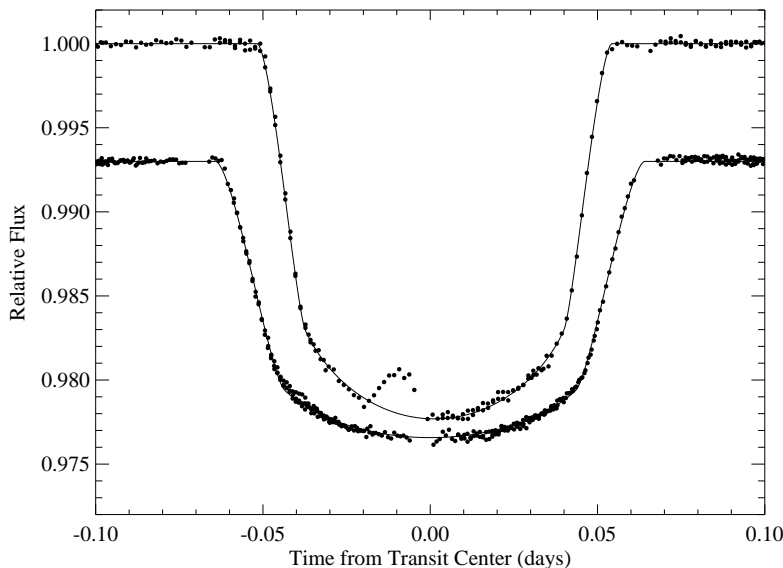


Fig. 2.— *HST* photometric light curves of transits of TrES-1 (top; *Brown et al., in preparation*) and HD 209458 (bottom; *Brown et al. 2001*, offset by -0.007 for clarity). The shorter orbital period and the smaller size of the TrES-1 star result in a transit that is shorter in duration than that of HD 209458. Similarly, the smaller star creates a deeper transit for TrES-1, despite the fact that HD 209458b is the larger planet; the planetary sizes also affect the duration of ingress and egress. The TrES-1 data reveal a “hump” centered at a time of -0.01 d. This is likely the result of the planet occulting a starspot (or complex of starspots) on the stellar surface.

constraint on the ratio R_{pl}/R_* . However, fits to such data exhibit a fundamental degeneracy amongst the parameters R_{pl} , R_* , and i , whereby the planet and stellar radii may be reduced in proportion so as to preserve the transit depth, and the orbital inclination may be correspondingly increased so as to conserve the chord length across the star. The uncertainty in R_{pl} is typically dominated by such degeneracies. Determining the value of R_{pl} requires fitting eclipse curves (facilitated by the analytic formulae of *Mandel and Agol, 2002*) subject to independent estimates of M_* , R_* , and the stellar limb-darkening coefficients. If sufficient photometric precision can be achieved, the value of R_* may be derived from the light curve itself. This results in a reduced uncertainty on the value of R_{pl} , due to its weaker dependence on M_* , ($\Delta R_{pl}/R_{pl} \simeq 0.3(\Delta M_*/M_*)$; see *Charbonneau (2003)*). For illustrative examples of the degeneracies that result from such fits, see *Winn et al. (2005)*, *Holman et al. (2005)*, and *Charbonneau et al. (2006)*.

HST has yielded spectacular transit light curves for two bright systems, HD 209458 (*Brown et al., 2001*) and TrES-1 (*Brown et al., in preparation*), which are shown in Fig. 2. The typical precision of these lightcurves is 10^{-4} per one-minute integration, sufficient to extract new information from relatively subtle properties of the light curve, such as the duration of the ingress and egress phases, and the curvature of the light curve near the transit center. In practice, such data have permitted a simultaneous fit that yields estimates of R_{pl} , R_* , i , and the stellar limb-darkening coefficients, thus reducing the number of assumed parameters

to one: M_* . *Cody and Sasselov (2002)* point out that the combined constraint on (M_*, R_*) is nearly orthogonal to that resulting from light-curve fitting, serving to reduce the uncertainty in R_{pl} . Further improvements can result from the simultaneously fitting of multi-color photometry under assumed values for the stellar-limb darkening, which serves to isolate the impact parameter (hence i) of the planet’s path across the star and break the shared degeneracy amongst R_{pl} , R_* , and i (*Jha et al., 2000; Deeg et al., 2001*). Recently, *Knutson et al. (2006)* have analyzed a spectrophotometric *HST* dataset spanning 290 – 1060 nm, and the combined effect of the constraints described above has been to permit the most precise determination of an exoplanet radius to date (HD 209458b; $R_{pl} = 1.320 \pm 0.025 R_{Jup}$).

2.1.5. Further Characterization Measurements. High-resolution stellar spectra obtained during transits can be used to determine the degree of alignment of the planet’s orbital angular momentum vector with the stellar spin axis. As the planet passes in front of the star, it produces a characteristic time-dependent shift of the photospheric line profiles that stems from occultation of part of the rotating stellar surface. This phenomenon is known as the Rossiter-McLaughlin effect (*Rossiter, 1924; McLaughlin, 1924*), and has long been observed in the spectra of eclipsing binary stars. *Queloz et al. (2000)* and *Bundy and Marcy (2000)* detected this effect during transits of HD 209458. A full analytic treatment of the phenomenon in the context of transiting extrasolar planets has been given by *Ohta et*

al. (2005). *Winn et al.* (2005) analyzed the extensive radial-velocity dataset of HD 209458, including 19 measurements taken during transit. They found that the measurements of the radial velocity of HD 209458 during eclipse exhibit an effective half-amplitude of $\Delta v \simeq 55 \text{ m s}^{-1}$, indicating a line-of-sight rotation speed of the star of $v \sin i_{\star} = 4.70 \pm 0.16 \text{ km s}^{-1}$. They also detected a small asymmetry in the Rossiter-McLaughlin anomaly, which they modeled as arising from an inclination, λ , of the planetary orbit relative to the apparent stellar equator of $\lambda = -4.4^{\circ} \pm 1.4^{\circ}$. Interestingly, this value is smaller than the $\lambda = 7^{\circ}$ tilt of the solar rotation axis relative to the net angular momentum vector defined by the orbits of the solar system planets (see *Beck and Giles*, 2005). *Wolf et al.* (2006) carried out a similar analysis for HD 149026, and found $\lambda = 12^{\circ} \pm 14^{\circ}$. For these planets, the timescales for tidal coplanarization of the planetary orbits and stellar equators are expected to be of order 10^{12} yr (*Winn et al.*, 2005; *Greenberg*, 1974; *Hut*, 1980), indicating that the observed value of λ likely reflects that at the end of the planet formation process.

Perturbations in the timing of planetary transits may be used to infer the presence of satellites or additional planetary companions (*Brown et al.*, 2001; *Miralda-Escudé*, 2002). *Agol et al.* (2005) and *Holman and Murray* (2005) have shown how non-transiting terrestrial-mass planets could be detected through timing anomalies. Although *HST* observations have yielded the most precise timing measurements to date (with a typical precision of 10s; see tabulation for HD 209458 in *Wittenmyer et al.*, 2005), the constraints from ground-based observations can nonetheless be used to place interesting limits on additional planets in the system, as was recently done for TrES-1 (*Steffen and Agol*, 2005).

Precise photometry can also yield surprises, as in the “hump” seen in Fig. 2. This feature likely results from the planet crossing a large sunspot (or a complex of smaller ones), and thus is evidence for magnetic activity on the surface of the star. Such activity may prove to be an important noise source for timing measurements of the sort just described, but it is also an interesting object of study in its own right, allowing periodic monitoring of the stellar activity along an isolated strip of stellar latitude (*Silva*, 2003).

2.2. Theory and Interpretation

2.2.1. Overview and Uncertainties. Transiting planets give us the opportunity to test our understanding of the physical structure of giant planets. In particular, structural models of the known transiting planets must be able to account for the wide range of radiation fluxes to which these planets are subjected, and they must recover the observed range of radii. In general, as the planetary mass decreases, a given external energy input has an increasingly larger influence on the size and interior structure of the planet. For hot Jupiters, the absorbed stellar flux creates a radiative zone in the subsurface regions that controls the planetary contraction, and ultimately dictates the radius. Models of transiting giant planets straddle the physical characteristics of brown

dwarfs and low-mass stars, as well as the solar system giants (for an overall review, see *Burrows et al.*, 2001).

The construction of structural models for giant planets is difficult because a number of key physical inputs are poorly constrained. This situation holds equally for extrasolar planets and for the exquisitely observed outer planets of the Solar system. A benefit of robust determinations of the parameters for a growing range of planets is that uncertain aspects of the theory can become increasingly constrained. Indeed, transit observations have the potential to clarify some of the core questions regarding giant planets.

The dominant uncertainty regarding the overall structure of gas giants is in the equation of state (see the review of *Guillot*, 2005). The interiors of solar system and extrasolar giant planets consist of partially degenerate, partially ionized atomic-molecular fluids (*Hubbard*, 1968). The pressure, P , in the interiors of most giant planets exceeds 10 Mbar, and central temperatures range from $T_c \simeq 10^4$ for Uranus and Neptune to $T_c \simeq 3 \times 10^4$ for objects such as HD 209458b. This material regime lies beyond the point where hydrogen ionizes and becomes metallic, although the details of the phase transition are still uncertain (*Saumon et al.*, 2000; *Saumon and Guillot*, 2004). The equation of state of giant planet interiors is partially accessible to laboratory experiments, including gas-gun (*Holmes et al.*, 1995), laser-induced shock compression (*Collins et al.*, 1998), pulsed-power shock compression (*Knudson et al.*, 2004), and convergent shock wave (*Boriskov et al.*, 2003) techniques. These experiments can achieve momentary pressures in excess of 1 Mbar, and they appear to be approaching the molecular to metallic hydrogen transition. Unfortunately, these experiments report diverging results. In particular, they yield a range of hydrogen compression factors relevant to planetary cores that differ by $\sim 50\%$. Furthermore, the laboratory experiments are in only partial agreement with first-principles quantum mechanical calculations of the hydrogen equation of state (*Militzer and Ceperley*, 2001; *Desjarlais*, 2003; *Bonev et al.*, 2004), and uncertainties associated with the equations of state of helium and heavier elements are even more severe (*Guillot*, 2005). At present, therefore, structural models must adopt the pragmatic option of choosing a thermodynamically consistent equation of state that reproduces either the high- or low-compression results (*Saumon and Guillot*, 2004).

Another uncertainty affecting the interior models is the existence and size of a radial region where helium separates from hydrogen and forms downward-raining droplets. The possibility that giant planet interiors are helium-stratified has non-trivial consequences for their structures, and ultimately, their sizes. In the case of Saturn, the zone of helium rain-out may extend all the way to the center, possibly resulting in a distinct helium shell lying on top of a heavier element core (*Fortney and Hubbard*, 2003).

Uncertainties in the equation of state, the bulk composition, and the degree of inhomogeneity allow for a depressingly wide range of models for the solar system giants that are consistent with the observed radii, surface tempera-

TABLE 1
PROPERTIES OF THE TRANSITING PLANETS

| Planet | M_\star M_\odot | P days | $T_{\text{eff},\star}$ K | R_\star R_\odot | R_{pl} R_{Jup} | M_{pl} M_{Jup} | $T_{\text{eq},pl}$ K | R_{pl} $20M_\oplus$ core | R_{pl} no core |
|--------------|------------------------|-------------|-----------------------------|------------------------|------------------------------|------------------------------|-------------------------|-------------------------------|---------------------|
| OGLE-TR-56b | $1.04 \pm .05$ | 1.21 | 5970 ± 150 | $1.10 \pm .10$ | $1.23 \pm .16$ | $1.45 \pm .23$ | 1800 ± 130 | $1.12 \pm .02$ | $1.17 \pm .02$ |
| OGLE-TR-113b | $0.77 \pm .06$ | 1.43 | 4752 ± 130 | $0.76 \pm .03$ | $1.08^{+.07}_{-.05}$ | $1.35 \pm .22$ | 1186 ± 78 | $1.07 \pm .01$ | $1.12 \pm .01$ |
| OGLE-TR-132b | $1.35 \pm .06$ | 1.69 | 6411 ± 179 | $1.43 \pm .10$ | $1.13 \pm .08$ | $1.19 \pm .13$ | 1870 ± 170 | $1.13 \pm .02$ | $1.18 \pm .02$ |
| HD 189733b | $0.82 \pm .03$ | 2.22 | 5050 ± 50 | $0.76 \pm .01$ | $1.15 \pm .03$ | $1.15 \pm .04$ | 1074 ± 58 | $1.07 \pm .01$ | $1.11 \pm .01$ |
| HD 149026b | $1.30 \pm .10$ | 2.88 | 6147 ± 50 | $1.45 \pm .10$ | $0.73 \pm .05$ | $0.36 \pm .03$ | 1533 ± 99 | $0.98 \pm .02$ | $1.15 \pm .02$ |
| TrES-1 | $0.87 \pm .03$ | 3.00 | 5214 ± 23 | $0.83 \pm .03$ | $1.12 \pm .04$ | $0.73 \pm .04$ | 1038 ± 61 | $1.02 \pm .01$ | $1.10 \pm .00$ |
| OGLE-TR-10b | $1.00 \pm .05$ | 3.10 | 6220 ± 140 | $1.18 \pm .04$ | $1.16 \pm .05$ | $0.54 \pm .14$ | 1427 ± 88 | $1.01 \pm .02$ | $1.13 \pm .01$ |
| HD 209458b | $1.06 \pm .13$ | 3.52 | 6099 ± 23 | $1.15 \pm .05$ | $1.32 \pm .03$ | $0.66 \pm .06$ | 1314 ± 74 | $1.02 \pm .01$ | $1.12 \pm .00$ |
| OGLE-TR-111b | $0.82^{+.15}_{-.02}$ | 4.02 | 5070 ± 400 | $0.85^{+.10}_{-.03}$ | $1.00^{+.13}_{-.06}$ | $0.53 \pm .11$ | 930 ± 100 | $0.97 \pm .02$ | $1.09 \pm .01$ |

tures, and gravitational moments. In particular (Saumon and Guillot, 2004), one can construct observationally-consistent models for Jupiter with core masses ranging from $0 - 12 M_\oplus$, and an overall envelope heavy-element content ranging from $6 - 37 M_\oplus$. This degeneracy must be broken in order to distinguish between the core accretion (Mizuno, 1980; Pollack et al., 1996; Hubickyj et al., 2004) and gravitational instability (Boss, 1997, 2000, 2004) hypotheses for planet formation. Fortunately, the growing dataset of observed masses and radii from the transiting extrasolar planets suggests a possible strategy for resolving the tangle of uncertainties. The extreme range of temperature conditions under which hot Jupiters exist, along with the variety of masses that are probed, can potentially provide definitive constraints on the interior structure of these objects.

2.2.2. Comparison to Observations. Following the discovery of 51 Pegb (Mayor and Queloz, 1995), models of Jovian-mass planets subject to strong irradiation were computed (Lin, Bodenheimer and Richardson, 1996; Guillot et al., 1996). These models predicted that short-period Jovian-mass planets with effective temperatures of roughly 1200 K would be significantly larger than Jupiter, and the discovery that HD 209458b has a large radius initially seemed to confirm these calculations. In general, R_{pl} is a weak function of planet mass, reflecting the overall $n = 1$ polytropic character of giant planets (Burrows et al., 1997, 2001).

In order to evaluate the present situation, we have collected the relevant quantities for the 9 transiting planets in Table 1. In particular, we list the most up-to-date estimates of P , R_\star , M_\star , R_{pl} , M_{pl} , as well as the stellar effective temperature, $T_{\text{eff},\star}$. We also list the value of the planetary equilibrium temperature, $T_{\text{eq},pl}$, which is calculated by assuming the value for the Bond albedo, A , recently estimated for TrES-1 ($A = 0.31 \pm 0.14$; Charbonneau et al., 2005; Section 3.2.3). The precision of the estimates of the physical properties varies considerably from star to star. By drawing from the Gaussian distributions corresponding to the uncertainties in Table 1 and the quoted value for A , we can estimate the uncertainty for M_{pl} and $T_{\text{eq},pl}$ for each planet.

Thereafter, for a particular choice of M_{pl} and $T_{\text{eq},pl}$, and fixing the planetary age at 4.5 Gyr, we can compute theoretical radii. For this task, we use the results of Bodenheimer et al. (2003), who computed models for insolated planets ranging in mass from $0.11 - 3.0 M_{\text{Jup}}$. To evaluate the radii differences that arise from different heavy element fractions, separate sequences were computed for models that contain and do not contain $20M_\oplus$ solid cores, and both predictions are listed in Table 1. The models have been calibrated so that, for the evolution of Jupiter up to the age of 4.5 Gyr, a model with a core gives the correct Jupiter radius to within 1%. Planetary age can also have a significant effect on R_{pl} . For example, the evolutionary models of Burrows et al. (2004) for OGLE-TR-56b ($1.45 M_{\text{Jup}}$) yield transit radii of $R_{pl} \simeq 1.5 R_{\text{Jup}}$ at 100 Myr, and $\sim 1.25 R_{\text{Jup}}$ after 2 Gyr. In general, however, R_{pl} evolves only modestly beyond the first 500 Myr, and hence the uncertainties in the ages of the parent stars (for which such young ages may generally be excluded) introduce errors of only a few percent into the values of R_{pl} .

The models use a standard Rosseland mean photospheric boundary condition, and as such, are primarily intended for cross-comparison of radii. The obtained planetary radii are, however, in excellent agreement with baseline models obtained by groups employing detailed frequency-dependent atmospheres (e.g. Burrows et al., 2004; Chabrier et al., 2004; Fortney et al., 2005b). The models assume that the surface temperature is uniform all the way around the planet, even though the rotation of the planet is likely tidally locked. Hydrodynamic simulations of the atmosphere that aim, in part, to evaluate the efficiency with which the planet redistributes heat from the dayside to the nightside have been performed by Cho et al. (2003), Showman and Guillot (2002), Cooper and Showman (2005), and Burkert et al. (2005) under various simplifying assumptions. There is no agreement on what the temperature difference between the dayside and the nightside should be (Section 3.2.4), and it depends on the assumed opacity in the atmosphere. Burkert et al. (2005) suggest that with a reasonable opacity, the difference could be 200 K, not enough to make an appreciable

difference in the radius.

A number of interesting conclusions regarding the bulk structural properties of the transiting planets can be drawn from Table 1. First, the baseline radius predictions display (1σ) agreement for seven of the nine known transiting planets. Second, the planets whose radii are in good agreement with the models span the full range of masses and effective temperatures. The models do not appear to be systematically wrong in some particular portion of parameter space. Although the reported accuracies of the basic physical parameters are noticeably worse for the OGLE systems than for the brighter targets, the constraints are nonetheless useful to address models of their physical structure and, in particular, the presence or absence of a solid core. Specifically, the baseline models in Table 1 indicate that the presence of a solid core in a $0.5 M_{\text{Jup}}$ planet with $T_{\text{eff},pl} = 1500$ K leads to a radius reduction of roughly $0.1 R_{\text{Jup}}$. This difference generally exceeds the uncertainty in the estimate of R_{pl} .

In the standard core-accretion paradigm for giant planet formation, as reviewed by *Lissauer* (1993), a Jovian planet arises from the collisional agglomeration of a solid $10\text{-}M_{\oplus}$ core over a period of several million years, followed by a rapid accretion of hundreds of Earth masses of nebular gas, lasting roughly 10^5 yr. The competing gravitational instability hypothesis (e.g. *Boss* 1997, 2004) posits that gas-giant planets condense directly from spiral instabilities in protostellar disks on a dynamical timescale of less than 10^3 yr. *Boss* (1998) points out that solid particles in the newly formed planet can precipitate to form a core during the initial contraction phase. Only 1% of the matter in the planet is condensible, however, so a Jovian-mass planet that formed by this process will have a core that is much less massive than one that formed by the core-accretion scenario.

Among the 7 planets that show agreement with the baseline models, it is presently difficult to discern the presence of a core. However, the “transit radius” effect (*Burrows et al.*, 2003; Section 2.2.3) will tend to systematically increase the observed radii above the model radii listed in Table 1 (which correspond to a 1-bar pressure level). Similarly, signal-to-noise-limited field transit surveys bias the mean radius of planets so detected to a value larger than that of the intrinsic population (*Gaudi*, 2005). Taking both effects into account lends favor to the models with cores. Clearly more transiting planets and more precise determinations of their properties are necessary, as are more physically detailed models. We note that the identification of lower-mass transiting planets (for which the effect of a solid core is prominent) would be particularly helpful to progress in these questions. Several groups (e.g. *Gould et al.*, 2003; *Hartman et al.*, 2005; *Pepper and Gaudi*, 2006) have considered the prospects for ground-based searches for planets with radii of that of Neptune, or less.

2.2.3. The Transit Radius Effect. When a planet occults its parent star, the wavelength-dependent value of R_{pl} so inferred is not necessarily the canonical planetary radius at a pressure level of 1 bar (*Lindal et al.*, 1981; *Hubbard et*

al., 2001), which we have used for the baseline predictions in Table 1. As such, the measured radius is approximately the impact parameter of the transiting planet at which the optical depth to the stellar light along a chord parallel to the star-planet line of centers is unity. This is not the optical depth in the radial direction, nor is it associated with the radius at the radiative-convective boundary. Hence, since the pressure level to which the transit beam is probing near the planet’s terminator is close to one millibar (*Fortney et al.*, 2003), there are typically 5 – 10 pressure scale heights difference between the measured value of R_{pl} and either the radiative-convective boundary (≥ 1000 bars) and the 1-bar radius. (If, as discussed in *Barman et al.* (2002), the transit radius is at pressures well below the 1 millibar level, then the effect would be even larger.) Furthermore, exterior to the radiative-convective boundary, the entropy is an increasing function of radius. One consequence of this fact is significant radial inflation vis à vis a constant entropy atmosphere. Both of these effects result in an apparent increase of perhaps $0.1 R_{\text{Jup}}$ ($\sim 7\%$) in the theoretical radius for HD 209458b and $0.05 R_{\text{Jup}}$ ($\sim 4\%$) for OGLE-TR-56b.

2.2.4. Explaining the Oddballs. Two of the planets, HD 209458b and HD 149026b, have radii that do not agree at all with the predictions. HD 209458b is considerably larger than predicted, and HD 149026b is too small. These discrepancies indicate that the physical structures of the transiting planets can depend significantly on factors other than M_{pl} and $T_{\text{eff},pl}$. It would appear that hot Jupiters are imbued with individual personalities.

While the radius of HD 209458b is certainly broadly consistent with a gas-giant composed primarily of hydrogen, studies by *Bodenheimer et al.* (2001) and *Guillot and Showman* (2002) were the first to make it clear that a standard model of a contracting, irradiated planet can recover $R_{pl} \simeq 1.35 R_{\text{Jup}}$ for HD 209458b only if the deep atmosphere is unrealistically hot. A number of resolutions to this conundrum have been suggested. *Bodenheimer et al.* (2001) argue that HD 209458b might be receiving interior tidal heating through ongoing orbital circularization. This hypothesis was refined by *Bodenheimer et al.* (2003), who computed grids of predicted planetary sizes under a variety of conditions, and showed that the then-current radial velocity data set for HD 209458b was consistent with the presence of an undetected planet capable of providing the requisite eccentricity forcing. The tidal-heating hypothesis predicts that HD 209458b is caught up in an anomalous situation, and that the majority of hot Jupiter-type planets will have considerably smaller radii than that observed for HD 209458b. Recent analyses by *Laughlin et al.* (2005b) and *Winn et al.* (2005) indicate that the orbital eccentricity of HD 209458b is close to zero. This conclusion is further buttressed by the timing of the secondary eclipse by *Deming et al.* (2005a; discussed in greater detail in Section 3.2.3), which places stringent upper limits on the eccentricity, except in the unlikely event that the orbit is precisely aligned to our line of sight. Thus the eccentricity appears to be be-

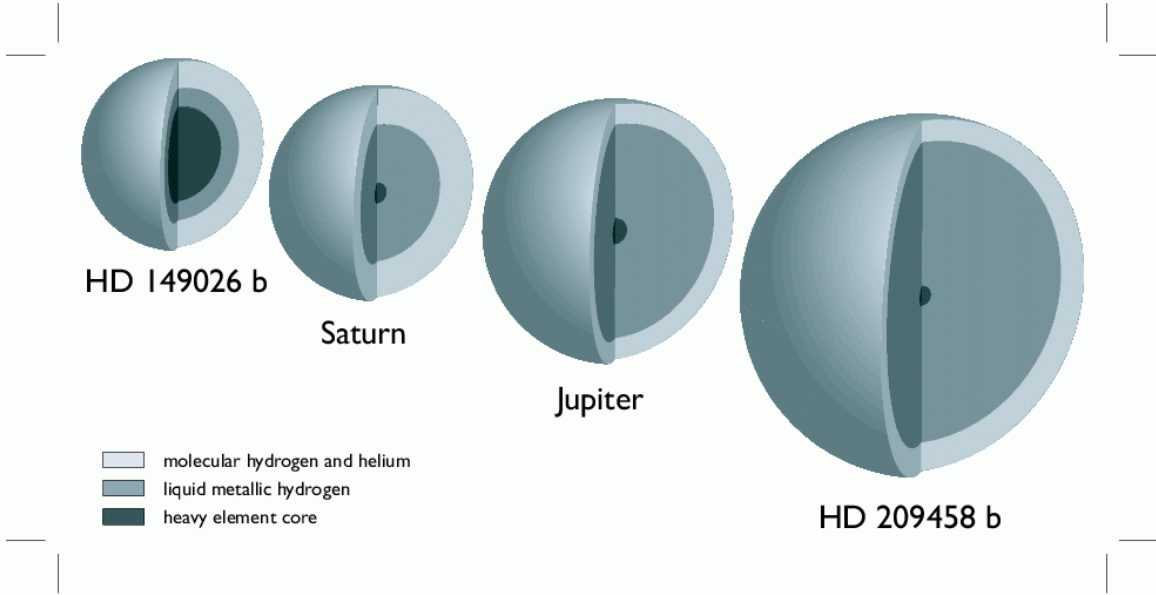


Fig. 3.— Cut-away diagrams of Jupiter, Saturn, and the two oddball extrasolar planets, drawn to scale. The observed radius of HD 149026b implies a massive core of heavy elements that makes up perhaps 70% of the planetary mass. In contrast, the radius of HD 209458b intimates a coreless structural model, as well as an additional energy source to explain its large value.

low the value required to generate sufficient tidal heating to explain the inflated radius.

Guillot and Showman (2002) proposed an alternate hypothesis in which strong insolation-driven weather patterns on the planet drive the conversion of kinetic energy into thermal energy at pressures of tens of bars. They explored this idea by modifying their planet evolution code to include a radially adjustable internal energy source term. They found that if kinetic wind energy is being deposited at adiabatic depths with an efficiency of 1%, then the large observed radius of the planet can be explained. Their hypothesis predicts that other transiting planets with similar masses and at similar irradiation levels should be similar in size to HD 209458b. The subsequent discovery that TrES-1 has a considerably smaller radius despite its similar temperature, mass, and parent star metallicity is evidence against the kinetic heating hypothesis, since it is not clear why this mechanism should act upon only HD 209458b.

Recently, an attractive mechanism for explaining the planet's large size has been advanced by *Winn and Holman* (2005) who suggest that the anomalous source of heat arises from obliquity tides that occur as a result of the planet being trapped in a Cassini state (e.g. *Peale*, 1969). In a Cassini state, a planet that is formed with a non-zero obliquity is driven during the course of spin synchronization to a final state in which spin precession resonates with orbital precession. When caught in a Cassini state, the planet is forced to maintain a non-zero obliquity, and thus experiences continued tidal dissipation as a result of orbital libration. Order-of-magnitude estimates indicate that the amount of expected tidal dissipation could generate enough heat to inflate the planet to the observed size.

HD 149026b presents a problem that is essentially the opposite to that of HD 209458b. Both the mass ($0.36 M_{\text{Jup}}$) and the radius ($0.73 R_{\text{Jup}}$) are considerably smaller than those of the other known transiting extrasolar planets. Curiously, HD 149026 is the only star of a transiting planet to have a metallicity that is significantly supersolar, $[\text{Fe}/\text{H}] = 0.36$. The observed radius is 30% smaller than the value predicted by the baseline model with a core of $20 M_{\oplus}$. Clearly, a substantial enrichment in heavy elements above solar composition is required. The mean density of the planet, 1.17 g cm^{-3} , is $1.7\times$ that of Saturn, which itself has roughly 25% heavy elements by mass. On the other hand, the planet is not composed entirely of water or silicates, or else the radius would be of order 0.4 or $0.28 R_{\text{Jup}}$, respectively (*Guillot et al.*, 1996, *Guillot* 2005). Models by *Sato et al.* (2005) and by *Fortney et al.* (2005b) agree that the observed radius can be recovered if the planet contains approximately $70 M_{\oplus}$ of heavy elements, either distributed throughout the interior or sequestered in a core.

The presence of a major fraction of heavy elements in HD 149026b has a number of potentially interesting ramifications for the theory of planet formation. *Sato et al.* (2005) argue that it would be difficult to form this giant planet by the gravitational instability mechanism (*Boss*, 2004). The large core also presents difficulties for conventional models of core accretion. In the core-accretion theory, which was developed in the context of the minimum-mass solar nebula, it is difficult to prevent runaway gas accretion from occurring onto cores more massive than $30 M_{\oplus}$, even if abundant in-falling planetesimals heat the envelope and delay the Kelvin-Helmholtz contraction that is required to let more gas into the planet's Hill sphere. The current structure

of HD 149026b suggests that it was formed in a gas-starved environment, yet presumably enough gas was present in the protoplanetary disk to drive migration from its probable formation region beyond 1 – 2 AU from the star inward to the current orbital separation of 0.043 AU. Alternately, a metal-rich disk would likely be abundant in planetesimals, which may in turn have promoted the inward migration of the planet via planetesimal scattering (*Murray et al.*, 1998).

3. ATMOSPHERES

By the standards of the Solar system, the atmospheres of the close-in planets listed in Table 1 are quite exotic. Located only 0.05 AU from their parent stars, these gas giants receive a stellar flux that is typically 10^4 that which strikes Jupiter. As a result, a flurry of theoretical activity over the past decade has sought to predict (and, more recently, interpret) the emitted and reflected spectra of these objects (e.g. *Seager and Sasselov*, 1998; *Seager et al.*, 2000; *Barman et al.*, 2001; *Sudarsky et al.*, 2003; *Allard et al.*, 2003; *Burrows et al.*, 2004; *Burrows*, 2005). Observations promise to grant answers to central questions regarding the atmospheres of the planets, including the identity of their chemical constituents, the presence (or absence) of clouds, the fraction of incident radiation that is absorbed (and hence the energy budget of the atmosphere), and the ability of winds and weather patterns to redistribute heat from the dayside to the nightside. For a detailed review of the theory of extrasolar planet atmospheres, see the chapter by *Marley et al.* We summarize the salient issues below (Section 3.1), and then proceed to discuss the successful observational techniques, and resulting constraints to date (Section 3.2).

3.1. Theory

3.1.1. Overview. In order to model the atmospheres and spectra of extrasolar giant planets in general, and hot Jupiters in particular, one must assemble extensive databases of molecular and atomic opacities. The species of most relevance, and which provide diagnostic signatures, are H_2O , CO , CH_4 , H_2 , Na , K , Fe , NH_3 , N_2 , and silicates. The chemical abundances of these and minority species are derived using thermochemical data and minimizing the global free energy. Non-equilibrium effects in the upper atmospheres require chemical networks and kinetic coefficients. With the abundances and opacities, as well as models for the stellar spectrum, one can embark upon calculations of the atmospheric temperature, pressure, and composition profiles and of the emergent spectrum of an irradiated planet. With atmospheric temperatures in the 1000 – 2000 K range, CO , not CH_4 , takes up much of the carbon in the low-pressure outer atmosphere, and N_2 , not NH_3 , sequesters most of the nitrogen. However, H_2O predominates in the atmospheres for both hot and cooler giants. Perhaps most striking in the spectrum of a close-in giant planet is the strong absorption due to the sodium and potassium resonance doublets. These lines are strongly pressure-broadened and likely dominate the visible spec-

tral region. The major infrared spectral features are due to H_2O , CO , CH_4 , and NH_3 . H_2 collision-induced absorption contributes very broad features in the infrared.

A self-consistent, physically realistic evolutionary calculation of the radius, $T_{\text{eff},pl}$, and spectrum of a giant planet in isolation requires an outer boundary condition that connects radiative losses, gravity (g), and core entropy (S). When there is no irradiation, the effective temperature determines both the flux from the core and the entire object. A grid of $T_{\text{eff},pl}$, g , and S , derived from detailed atmosphere calculations, can then be used to evolve the planet (e.g. *Burrows et al.*, 1997; *Allard et al.*, 1997). However, when a giant planet is being irradiated by its star, this procedure must be modified to include the outer stellar flux in the calculation that yields the corresponding S - $T_{\text{eff},pl}$ - g relationship. This must be done for a given external stellar flux and spectrum, which in turn depends upon the stellar luminosity spectrum and the orbital distance of the giant planet. Therefore, one needs to calculate a new S - $T_{\text{eff},pl}$ - g grid under the irradiation regime of the hot Jupiter that is tailor-made for the luminosity and spectrum of its primary and orbital distance. With such a grid, the radius evolution of a hot Jupiter can be calculated, with its spectrum as a by-product.

3.1.2. The Day-Night Effect and Weather. A major issue is the day-night cooling difference. The gravity and interior entropy are the same for the day and the night sides. For a synchronously rotating hot Jupiter, the higher core entropies needed to explain a large measured radius imply higher internal fluxes on a night side if the day and the night atmospheres are not coupled (e.g. *Guillot and Showman*, 2002). For strongly irradiated giant planets, there is a pronounced inflection and flattening in the temperature-pressure profile that is predominantly a result of the near balance at some depth between countervailing incident and internal fluxes. The day-side core flux is suppressed by this flattening of the temperature gradient and the thickening of the radiative zone due to irradiation. However, *Showman and Guillot* (2002), *Menou et al.* (2003), *Cho et al.* (2003), *Burkert et al.* (2005), and *Cooper and Showman* (2005) have recently demonstrated that strong atmospheric circulation currents that advect heat from the day to the night sides at a wide range of pressure levels are expected for close-in giant planets. *Showman and Guillot* (2002) estimate that below pressures of 1 bar the night-side cooling of the air can be quicker than the time it takes the winds to traverse the night side, but that at higher pressures the cooling timescale is far longer. Importantly, the radiative-convective boundary in a planet such as HD 209458b is very deep, at pressures of perhaps 1000 bar. This may mean that due to the coupling of the day and the night sides via strong winds at depth, the temperature-pressure profiles at the convective boundary on both sides are similar. This would imply that the core cooling rate is roughly the same in both hemispheres. Since the planet brightness inferred during secondary eclipse (Section 3.2.3) depends upon the advection of stellar heat to the night side, such data can provide constraints on the meteo-

rology and general circulation models.

Almost complete redistribution of heat occurs in the case of Jupiter, where the interior flux is latitude- and longitude-independent. However, the similarity in Jupiter of the day and night temperature-pressure profiles and effective temperatures is a consequence not of the redistribution of heat by rotation or zonal winds, but of the penetration into the convective zone on the day side of the stellar irradiation (Hubbard, 1977). Core convection then redistributes the heat globally and accounts for the uniformity of the temperature over the entire surface. Therefore, whether direct heating of the convective zone by the stellar light is responsible, as it is in our own Jovian planets, for the day-night smoothing can depend on the ability of the stellar insolation to penetrate below the radiative-convective boundary. This does not happen for a hot Jupiter. Clearly, a full three-dimensional study will be required to definitively resolve this thorny issue.

Clouds high in the atmospheres of hot Jupiters with $T_{\text{eff},pl} > 1500$ K would result in wavelength-dependent flux variations. Cloud opacity tends to block the flux windows between the molecular absorption features, thereby reducing the flux peaks. Additionally, clouds reflect some of the stellar radiation, increasing the incident flux where the scattering opacity is high. This phenomenon tends to be more noticeable in the vicinity of the gaseous absorption troughs.

3.2. Observations

The direct study of extrasolar planets orbiting mature (Gyr) Sun-like stars may proceed without the need to image the planet (i.e. to spatially separate the light of the planet from that of the star). Indeed, this technical feat has not yet been accomplished. Rather, the eclipsing geometry of transiting systems permits the spectrum of the planet and star to be disentangled through monitoring of the variation in the combined system light as a function of the known orbital phase. Detections and meaningful upper limits have been achieved using the following three techniques.

3.2.1. Transmission Spectroscopy. The technique of transmission spectroscopy seeks to ratio stellar spectra gathered during transit with those taken just before or after this time, the latter providing a measurement of the spectrum of the isolated star. Wavelength-dependent sources of opacity in the upper portions of the planetary atmosphere, or in its exosphere, will impose absorption features that could be revealed in this ratio. This technique can be viewed as probing the wavelength-dependent variations in the inferred value of R_{pl} .

The first composition signature (Charbonneau *et al.*, 2002) was detected with the *HST* STIS spectrograph. The team measured an increase in the transit depth of $(2.32 \pm 0.57) \times 10^{-4}$ for HD 209458 in a narrow bandpass centered on the sodium resonance lines near 589 nm. Ruling out alternate explanations of this diminution, they conclude that the effect results from absorption due to atomic sodium

in the planetary atmosphere, which indeed had been unanimously predicted to be a very prominent feature at visible wavelengths (Seager and Sasselov, 2000; Hubbard *et al.*, 2001; Brown, 2001). Interestingly, the detected amplitude was roughly 1/3 that predicted by baseline models that incorporated a cloudless atmosphere and a solar abundance of sodium in atomic form. Deming *et al.* (2005b) follow the earlier work of Brown *et al.* (2002) to achieve strong upper limits on the CO bandhead at $2.3 \mu\text{m}$. Taken together, the reduced amplitude of the sodium detection and the upper limits on CO suggest the presence of clouds high in the planetary atmosphere (e.g. Fortney *et al.*, 2003), which serve to truncate the effective size of the atmosphere viewed in transmission. Fortney (2005) considers the slant optical depth and shows that even a modest abundance of condensates or hazes can greatly reduce the size of absorption features measured by this technique. Alternately, non-LTE effects may explain the weaker-than-expected sodium feature (Barman *et al.*, 2005).

Planetary exospheres are amenable to study by this method, as the increased cross-sectional area (compared to the atmospheres) implies a large potential signal. Vidal-Madjar *et al.* (2003) observed a $15 \pm 4\%$ transit depth of HD 209458 when measured at $\text{Ly}\alpha$. The implied physical radius exceeds the Roche limit, leading them to conclude that material is escaping the planet (Lecavelier des Etangs *et al.*, 2004; Baraffe *et al.*, 2004). However, the minimum escape rate required by the data is low enough to reduce the planetary mass by only 0.1% over the age of the system. More recently, Vidal-Madjar *et al.* (2004) have claimed detection of other elements, with a lower statistical significance. Significant upper limits on various species at visible wavelengths have been presented by Bundy and Marcy (2000), Moutou *et al.* (2001, 2003), Winn *et al.* (2004), and Narita *et al.* (2005).

3.2.2 Reflected Light. Planets shine in reflected light with a visible-light flux f_{pl} (relative to that of their stars, f_{\star}) of

$$\left(\frac{f_{pl}}{f_{\star}}\right)_{\lambda}(\alpha) = \left(\frac{R_{pl}}{a}\right)^2 p_{\lambda} \Phi_{\lambda}(\alpha),$$

where a is the orbital separation, p_{λ} is the geometric albedo, and $\Phi_{\lambda}(\alpha)$ is the phase function, which describes the relative flux at a phase angle α to that at opposition. Even assuming an optimistic values for p_{λ} , hot Jupiters present a flux ratio of less than 10^{-4} that of their stars. See Marley *et al.* (1999), Seager *et al.* (2000) and Sudarsky *et al.* (2000) for theoretical predictions of the reflection spectra and phase functions of hot Jupiters.

The first attempts to detect this modulation adopted a spectroscopic approach, whereby a series of spectra spanning key portions of the orbital phase are searched for the presence of a copy of the stellar spectrum. For non-transiting systems, this method is complicated by the need to search over possible values of the unknown orbital inclination. The secondary spectrum should be very well sep-

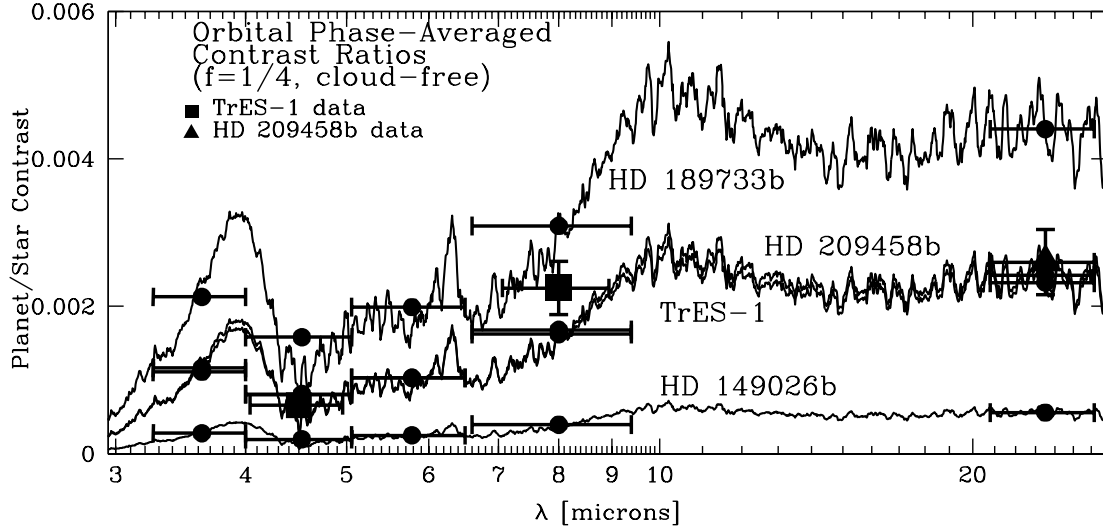


Fig. 4.— The orbital phase-averaged planet-to-star flux-density ratio as a function of wavelength (λ , in μm) for the models of the four known transiting extrasolar planets for which such observations might be feasible (Burrows *et al.*, 2005, and *in preparation*). The bandpass-integrated predicted values are shown as filled circles, with the bandwidths indicated by horizontal bars. The measured values for TrES-1 at 4.5 μm and 8.0 μm (Charbonneau *et al.*, 2005) are shown as filled squares, and the observed value at 24 μm for HD 209458b (Deming *et al.*, 2005a) is shown as a filled triangle. The extremely favorable contrast for HD 189733, and the extremely challenging contrast ratio for HD 149026, both result primarily from the respective planet-to-star surface area ratios.

arated spectroscopically, as the orbital velocities for these hot Jupiters are typically 100 km s^{-1} , much greater than the typical stellar line widths of $< 15 \text{ km s}^{-1}$. Since the method requires multiple high signal-to-noise ratio, high-dispersion spectra, only the brightest systems have been examined. A host of upper limits have resulted for several systems (e.g. Charbonneau *et al.*, 1999; Collier Cameron *et al.*, 2002; Leigh *et al.*, 2003a, 2003b), typically excluding values of $p_\lambda > 0.25$ averaged across visible wavelengths. These upper limits assume a functional dependence for $\Phi_\lambda(\alpha)$ as well as a gray albedo, i.e. that the planetary spectrum is a reflected copy of the stellar spectrum.

Space-based platforms afford the opportunity to study the albedo and phase function in a straightforward fashion by seeking the photometric modulation of the system light. The MOST satellite (Walker *et al.*, 2003) should be able to detect the reflected light from several hot Jupiters (Green *et al.*, 2003), or yield upper limits that will severely constrain the atmospheric models, and campaigns on several systems are completed or planned. The upcoming Kepler Mission (Borucki *et al.*, 2003) will search for this effect, and should identify 100 – 760 non-transiting hot Jupiters with orbital periods of $P < 7 \text{ d}$ (Jenkins and Doyle, 2003).

3.2.3. Infrared Emission. At infrared wavelengths, the secondary eclipse (i.e. the decrement in the system flux due to the passage of the planet behind the star) permits a determination of the planet-to-star brightness ratio. Since the

underlying stellar spectrum may be reliably assumed from stellar models (e.g. Kurucz, 1992), such estimates afford the first direct constraints on the emitted spectra of planets orbiting other Sun-like stars. In the Rayleigh-Jeans limit, the ratio of the planetary flux to that of the star is

$$\left(\frac{f_{pl}}{f_\star}\right) \simeq \frac{T_{eq,pl}}{T_{eff,\star}} \left(\frac{R_{pl}}{R_\star}\right)^2.$$

The last factor is simply the transit depth. From Table 1, we can see that the typical ratio of stellar to planetary temperatures is $3.5 - 5.5$, leading to predicted secondary eclipse amplitudes of several millimagnitudes.

Charbonneau *et al.* (2005) and Deming *et al.* (2005a) have recently employed the remarkable sensitivity and stability of the *Spitzer Space Telescope* to detect the thermal emission from TrES-1 (4.5 μm and 8.0 μm) and HD 209458b (24 μm); Fig. 4. These measurements provide estimates of the planetary brightness temperatures in these 3 bands, which in turn can be used to estimate (under several assumptions) the value of $T_{eq,pl}$ and A of the planets. Observations of these two objects in the other *Spitzer* bands shown in Fig. 4 (as well as the 16 μm photometric band of the IRS peak-up array) are feasible. Indeed, at the time of writing, partial datasets have been gathered for all four planets shown in Fig. 4. The results should permit a detailed search for the presence of spectroscopically-dominant molecules, notably, CH_4 , CO , and H_2O . Using the related technique of occultation spectroscopy, Richard-

son *et al.* (2003a, 2003b) have analyzed a series of infrared spectra spanning a time before, during, and after secondary eclipse, and present useful upper limits on the presence of planetary features due to these molecules.

Williams *et al.* (2006) have outlined a technique by which the spatial dependence of the planetary emission could be resolved in longitude through a careful monitoring of the secondary eclipse. Such observations, as well as attempts to measure the phase variation as the planet orbits the star (and hence presents a different face to the Earth) are eagerly anticipated to address numerous models of the dynamics and weather of these atmospheres (Section 3.1.2).

The elapsed time between the primary and secondary eclipse affords a stringent upper limit on the quantity $e \cos \varpi$, and the relative durations of the two events constrains $e \sin \varpi$ (Kallrath and Milone 1999; Charbonneau 2003). The resulting limits on e are of great interest in gauging whether tidal circularization is a significant source of energy for the planet (Section 2.2.4).

3.2.4. Inferences from the Infrared Detections. Varying planet mass, planet radius, and stellar mass within their error bars alters the resulting predicted average planet-star flux ratios only slightly (Burrows *et al.*, 2005). Similarly, and perhaps surprisingly, adding Fe and forsterite clouds does not shift the predictions in the Spitzer bands by an appreciable amount. Moreover, despite the more than a factor of two difference in the stellar flux at the planet, the predictions for the planet-star ratios for TrES-1 and HD209458b are not very different. Fortney *et al.* (2005b) explore the effect of increasing the metallicity of the planets, and find a better agreement to the red 4.5/8.0 μm color of TrES-1 with a enrichment factor of 3 – 5. Seager *et al.* (2005) show that models with an increased carbon-to-oxygen abundance produce good fits to the HD 209458b data, but conclude that a wide range of models produce plausible fits. Barman *et al.* (2005) examine the effect of varying the efficiency for the redistribution of heat from the dayside to the nightside, and find evidence that models with significant redistribution (and hence more isotropic temperatures) are favored.

In Fig. 4, there is a hint of the presence of H_2O , since it is expected to suppress flux between 4 – 10 μm . This is shortward of the predicted 10 μm peak in planet-star flux ratio, which is due to water’s relative abundance and the strength of its absorption bands in that wavelength range. Without H_2O , the fluxes in the 3.6 – 8.0 μm bands would be much greater. Hence, a comparison of the TrES-1 and HD 209458b data suggests, but does not prove, the presence of water. Seeing (or excluding) the expected slope between the 5.8 μm and 8.0 μm bands and the rise from 4.5 μm to 3.6 μm would be more revealing in this regard. Furthermore, the relative strength of the 24 μm flux ratio in comparison with the 3.6 μm , 4.5 μm , and 5.8 μm channel ratios is another constraint on the models, as is the closeness of the 8.0 μm and 24 μm ratios. If CH_4 is present in abundance, then the 3.6 μm band will test this. However, the preliminary conclusion for these close-in Jupiters is that

CH_4 should not be in evidence. Models have difficulty fitting the precise depth of the 4.5 μm feature for TrES-1. It coincides with the strong CO absorption predicted to be a signature of hot Jupiter atmospheres. However, the depth of this feature is only a weak function of the CO abundance. A CO abundance $100\times$ larger than expected in chemical equilibrium lowers this flux ratio at 4.5 μm by only $\sim 25\%$. Therefore, while the 4.5 μm data point for TrES-1 implies that CO has been detected, the exact fit is problematic.

In sum, *Spitzer* observations of the secondary eclipses of the close-in transiting giant planets will provide information on the presence of CO and H_2O in their atmospheres, as well as on the role of clouds in modifying the planet-to-star flux ratios over the 3 – 25 μm spectral range. Furthermore, there is good reason to believe that the surface elemental abundances of extrasolar giant planets are not the same as the corresponding stellar elemental abundances, and *Spitzer* data across the available bandpasses will soon better constrain the atmospheric metallicities and C/O ratios of these planets. Moreover, and most importantly, the degree to which the heat deposited by the star on the day side is advected by winds and jet streams to the night side is unknown. If this transport is efficient, the day-side emissions probed during secondary eclipse will be lower than the case for inefficient transport. There is already indication in the data for HD 209458b and TrES-1 that such transport may be efficient (e.g. Barman *et al.*, 2005), but much more data are needed to disentangle the effects of the day-night heat redistribution, metallicity, and clouds and to identify the diagnostic signatures of the climate of these extrasolar giant planets. The recently detected hot Jupiter, HD 189733b (Bouchy *et al.*, 2005a) is a veritable goldmine for such observations (Fig. 4), owing to the much greater planet-to-star contrast ratio.

4. FUTURE PROSPECTS

With the recent radial-velocity discoveries of planets with masses of 7 – 20 M_\oplus (e.g. Bonfils *et al.* 2005; Butler *et al.*, 2004; McArthur *et al.*, 2004; Rivera *et al.*, 2005; Santos *et al.*, 2004), the identification of the first such object in a transiting configuration is eagerly awaited. The majority of these objects have been found in orbit around low-mass stars, likely reflecting the increased facility of their detection for a fixed Doppler precision. Despite the smaller expected planetary size, the technical challenge of measuring the transits will be alleviated by the smaller stellar radius, which will serve to make the transits deep (but less likely to occur). Due to the low planetary mass, the influence of a central core (Section 2.2.2) will be much more prominent. Furthermore, the reduced stellar size and brightness implies that atmospheric observations (Section 3.2) will be feasible. The radial-velocity surveys monitor few stars later than M4V, but transiting planets of even later spectral types could be identified by a dedicated photometric monitoring campaign of several thousand of the nearest targets. An Earth-sized planet orbiting a late M-dwarf with a week-long

period would lie within the habitable zone and, moreover, it would present the same infrared planet-to-star brightness ratio as that detected (Section 3.2.3). We note the urgency of locating such objects (should they exist), due to the limited cryogenic lifetime of *Spitzer*.

The excitement with which we anticipate the results from the *Kepler* (Borucki et al., 2003) and *COROT* (Baglin, 2003) missions cannot be overstated. These projects aim to detect scores of rocky planets transiting Sun-like primaries, and the *Kepler Mission* in particular will be sensitive to year-long periods and hence true analogs of the Earth. Although direct follow-up of such systems (Section 3.2) with extant facilities appears precluded by signal-to-noise considerations, future facilities (notably the *James Webb Space Telescope*) may permit some initial successes.

We conclude that the near-future prospects for studies of transiting planets are quite bright (although they may dim, periodically), and we anticipate that the current rapid pace of results will soon eclipse this review – just in time for Protostars and Planets VI.

Acknowledgments. AB acknowledges support from NASA through grant NNG04GL22G. GL acknowledges support from the NASA OSS and NSF CAREER programs. We thank Scott Gaudi for illuminating suggestions.

REFERENCES

- Agol E., Steffen J., Sari R., and Clarkson W. (2005) *Mon. Not. R. Astron. Soc.*, 359, 567-579.
- Allard F., Hauschildt P. H., Alexander D. R., and Starrfield, S. (1997) *Ann. Rev. Astron. Astrophys.*, 35, 137-177.
- Allard F., Baraffe I., Chabrier G., Barman T. S., and Hauschildt P. H. (2003) In *Scientific Frontiers in Research on Extrasolar Planets* (D. Deming and S. Seager, eds.), pp. 483-490. ASP Conf. Series, San Francisco.
- Alonso R. (2005) *Ph.D. Thesis*, University of La Laguna.
- Alonso R., Brown T. M., Torres, G., Latham D. W., Sozzetti A., et al. (2004) *Astrophys. J.*, 613, L153-L156.
- Baglin A. (2003) *Adv. Space Res.*, 31, 345-349.
- Bakos G., Noyes R. W., Kovács G., Stanek K. Z., Sasselov D. D., et al. (2004) *Publ. Astron. Soc. Pac.*, 116, 266-277.
- Baraffe I., Selsis F., Chabrier G., Barman T. S., Allard F., et al. (2004) *Astron. Astrophys.*, 419, L13-L16.
- Barman T. S., Hauschildt P. H., and Allard F. (2001) *Astrophys. J.*, 556, 885-895.
- Barman T. S., Hauschildt P. H., Schweitzer A., Stancil P. C., Baron E., et al. (2002), *Astrophys. J.*, 569, L51-L54.
- Barman T. S., Hauschildt P. H., and Allard F. (2005), *Astrophys. J.*, 632, 1132-1139.
- Beck J. G. and Giles P. (2005) *Astrophys. J.*, 621, L153-L156.
- Bodenheimer P., Lin D. N. C., and Mardling R. A. (2001) *Astrophys. J.*, 548, 466-472.
- Bodenheimer P., Laughlin G., and Lin D. N. C. (2003) *Astrophys. J.*, 592, 555-563.
- Bonev G. V., Militzer B., and Galli G. (2004) *Phys. Rev. B*, 69, 014101.
- Bonfils X., Forveille T., Delfosse X., Udry S., Mayor M., et al. (2005) *Astron. Astrophys.*, 443, L15-L18.
- Boriskov G. V. et al. (2003) *Dokl. Phys.* 48, 553-555.
- Borucki W. J., Caldwell D., Koch D. G., Webster L. D., Jenkins J. M., et al. (2001) *Publ. Astron. Soc. Pac.*, 113, 439-451.
- Borucki W. J., Koch D. G., Lissauer J. J., Basri G. B., Caldwell J. F., et al. (2003) *Proc. SPIE*, 4854, 129-140.
- Boss A. P. (1997) *Science*, 276, 1836-1839.
- Boss A. P. (1998) *Astrophys. J.*, 503, 923-937.
- Boss A. P. (2000) *Astrophys. J.*, 536, L101-L104.
- Boss A. P. (2004) *Astrophys. J.*, 610, 456-463.
- Bouchy F., Pont F., Santos N. C., Melo C., Mayor M., et al. (2004) *Astron. Astrophys.*, 421, L13-L16.
- Bouchy F., Udry S., Mayor M., Pont F., Iribarne N., et al. (2005a) *Astron. Astrophys.*, 444, L15-L19.
- Bouchy F., Pont F., Melo C., Santos N. C., Mayor M., et al. (2005b) *Astron. Astrophys.*, 431, 1105-1121.
- Brown T. M. (2001), *Astrophys. J.*, 553, 1006-1026.
- Brown T. M. (2003) *Astrophys. J.*, 593, L125-L128.
- Brown T. M. and Charbonneau D. (2000). In *Disks, Planetesimals, and Planets* (F. Garzón et al., eds.), pp. 584-589. ASP Conf. Series, San Francisco.
- Brown T. M., Charbonneau D., Gilliland R. L., Noyes R. W., and Burrows A. (2001) *Astrophys. J.*, 551, 699-709.
- Brown T. M., Libbrecht K. G., and Charbonneau D. (2002), *Publ. Astron. Soc. Pac.*, 114, 826-832.
- Bundy K. A. and Marcy G. W. (2000), *Publ. Astron. Soc. Pac.*, 112, 1421-1425.
- Burke C. J., Gaudi B. S., DePoy D. L., Pogge R. W., and Pinsonneault M. H. (2004), *Astron. J.*, 127, 2382-2397.
- Burkert A., Lin D. N. C., Bodenheimer P. H., Jones C. A., and Yorke H. W. (2005) *Astrophys. J.*, 618, 512-523.
- Burrows A. (2005) *Nature*, 433, 261-268.
- Burrows A., Marley M., Hubbard W. B., Lunine J. I., Guillot T., et al. (1997) *Astrophys. J.*, 491, 856-875.
- Burrows A., Hubbard W. B., Lunine J. I., and Liebert J. (2001) *Rev. Mod. Phys.*, 73, 719-765.
- Burrows A., Sudarsky D., and Hubbard W. B. (2003) *Astrophys. J.*, 594, 545-551.
- Burrows A., Hubeny I., Hubbard W. B., Sudarsky D., and Fortney J. J. (2004) *Astrophys. J.*, 610, L53-L56.
- Burrows A., Sudarsky D., and Hubeny I. (2004) *Astrophys. J.*, 609, 407-416.
- Burrows A., Hubeny I., and Sudarsky D. (2005) *Astrophys. J.*, 625, L135-L138.
- Butler R. P., Vogt S. S., Marcy G. W., Fischer D. A., Wright J. T., et al. (2004) *Astrophys. J.*, 617, 580-588.
- Chabrier G., Barman T., Baraffe I., Allard F., and Hauschildt P. H. (2004) *Astrophys. J.*, 603, L53-L56.
- Charbonneau D. (2003) In *Scientific Frontiers in Research on Extrasolar Planets* (D. Deming and S. Seager, eds.), pp. 449-456. ASP Conf. Series, San Francisco.
- Charbonneau D., Noyes R. W., Korzennik S. G., Nisenson P., Jha S., et al. (1999) *Astrophys. J.*, 522, L145-L148.
- Charbonneau D., Brown T. M., Latham D. W., and Mayor M. (2000) *Astrophys. J.*, 529, L45-L48.
- Charbonneau D., Brown T. M., Noyes R. W., and Gilliland R. L. (2002) *Astrophys. J.*, 568, 377-384.
- Charbonneau D., Brown T. M., Dunham E. W., Latham D. W., Looper D. L., et al. (2004) In *The Search for Other Worlds* (S. Holt and D. Deming, eds.), pp. 151-160. AIP Conf. Series.
- Charbonneau D., Allen, L. E., Megeath S. T., Torres G., Alonso R., et al. (2005) *Astrophys. J.*, 626, 523-529.
- Charbonneau D., Winn J. N., Latham D. W., Bakos G., Falco E., et al. (2006), *Astrophys. J.*, 636, 445-452.

- Cho J. Y.-K., Menou K., Hansen B. M. S., and Seager S. (2003) *Astrophys. J.*, 587, L117-L120.
- Christian D. J., Pollacco D. L., Clarkson W. I., Collier Cameron A., Evans N., et al. (2004) In *The 13th Cool Stars Workshop* (F. Favata, ed.). ESA Spec. Pub. Series.
- Cody A. M. and Sasselov D. D. (2002) *Astrophys. J.*, 569, 451-458.
- Collier Cameron A., Horne K., Penny A., and Leigh C. (2002), *Mon. Not. R. Astron. Soc.*, 330, 187-204.
- Collins G. W., d Silva L. B., Celliers P., et al. (1998) *Science*, 281, 1178-1181.
- Cooper C. S. and Showman A. P. (2005) *Astrophys. J.*, 629, L45-L48.
- da Silva R., Udry S., Bouchy F., Mayor M., Moutou C., et al. (2006) *Astron. Astrophys.*, 446, 717-722.
- Deeg H. J., Garrido R., and Claret A. (2001) *New Astronomy*, 6, 51-60.
- Deeg H. J., Alonso R., Belmonte J. A., Alsubai K., Horne K., et al. (2004) *Publ. Astron. Soc. Pac.*, 116, 985-995.
- Deming D., Seager S., Richardson L. J., and Harrington J. (2005a) *Nature*, 434, 740-743.
- Deming D., Brown T. M., Charbonneau D., Harrington J., and Richardson L. J. (2005b), *Astrophys. J.*, 622, 1149-1159.
- Desjarlais M. P. (2003) *Phys. Rev. B*, 68, 064204.
- Drake A. J. (2003) *Astrophys. J.*, 589, 1020-1026.
- Dreizler S., Rauch T., Hauschildt P., Schuh S. L., Kley W., et al. (2002) *Astron. Astrophys.*, 391, L17-L20.
- Dunham E. W., Mandushev G. I., Taylor B. W., and Oetiker B. (2004) *Publ. Astron. Soc. Pac.*, 116, 1072-1080.
- Fischer D., Laughlin G., Butler R. P., Marcy G., Johnson J., et al. (2005) *Astrophys. J.*, 620, 481-486.
- Fortney, J. J. (2005) *Mon. Not. R. Astron. Soc.*, 364, 649-653.
- Fortney J. J. and Hubbard W. B. (2003) *Icarus*, 164, 228-243.
- Fortney J. J., Sudarsky D., Hubeny I., Cooper C. S., Hubbard W. B., et al. (2003) *Astrophys. J.*, 589, 615-622.
- Fortney J. J., Marley M. S., Lodders K., Saumon D., and Freedman R. S. (2005a) *Astrophys. J.*, 627, L69-L72.
- Fortney J. J., Saumon D., Marley M. S., Lodders K., and Freedman R. (2005b) *Astrophys. J.*, in press.
- Gaudi B. S. (2005) *Astrophys. J.*, 628, L73-L76.
- Gaudi B. S., Seager S., and Mallen-Ornelas G. (2005) *Astrophys. J.*, 623, 472-481.
- Gilliland R. L., Brown T. M., Guhathakurta P., Sarajedini A., Milone E. F., et al. (2000) *Astrophys. J.*, 545, L47-L51.
- Girardi L., Bertelli G., Bressan A., Chiosi C., Groenewegen M. A. T., et al. (2002) *Astron. Astrophys.*, 391, 195-212.
- Gould A., Pepper J., and DePoy D. L. (2003) *Astrophys. J.*, 594, 533-537.
- Green D., Matthews J., Seager S., and Kuschnig R. (2003) *Astrophys. J.*, 597, 590-601.
- Greenberg R. (1974) *Icarus*, 23, 51-58.
- Guillot T. (2005) *Ann. Rev. Earth Planet. Sci.*, 33, 493-530.
- Guillot T. and Showman A. P. (2002) *Astron. Astrophys.*, 385, 156-165.
- Guillot T., Burrows A., Hubbard W. B., Lunine J. I., and Saumon D. (1996) *Astrophys. J.*, 459, L35-L38.
- Hartman J. D., Stanek K. Z., Gaudi B. S., Holman M. J., and McLeod B. A. (2005) *Astron. J.*, 130, 2241-2251.
- Henry G. W., Marcy G. W., Butler R. P., and Vogt S. S. (2000) *Astrophys. J.*, 529, L41-L44.
- Holman M. J. and Murray N. W. (2005) *Science*, 307, 1288-1291.
- Holman M. J., Winn J. N., Stanek K. Z., Torres G., Sasselov D. D., et al. (2005) *Astrophys. J.*, submitted.
- Holmes N. C., Ross M., and Nellis W. J. (1995) *Phys. Rev. B.*, 52, 15835-15845.
- Hubbard W. B. (1968) *Astrophys. J.*, 152, 745-754.
- Hubbard W. B. (1977) *Icarus*, 30, 305-310.
- Hubbard W. B., Fortney J. J., Lunine J. I., Burrows A., Sudarsky D., et al. (2001) *Astrophys. J.*, 560, 413-419.
- Hubickyj O., Bodenheimer P., and Lissauer J. J. (2004) In *Gravitational Collapse: From Massive Stars to Planets* (G. García-Segura et al., eds), pp. 83-86. Rev. Mex. Astron. Astrophys. Conf. Series.
- Hut P. (1980) *Astron. Astrophys.*, 92, 167-170.
- Janes K. (1996) *J. Geophys. Res.*, 101, 14853-14860.
- Jenkins J. M. and Doyle L. R. (2003) *Astrophys. J.*, 595, 429-445.
- Jenkins J. M., Caldwell D. A., and Borucki W. J. (2002) *Astrophys. J.*, 564, 495-507.
- Jha S., Charbonneau D., Garnavich P. M., Sullivan D. J., Sullivan T., et al. (2000) *Astrophys. J.*, 540, L45-L48.
- Kallrath J. and Milone E. F. (1999) In *Eclipsing Binary Stars: Modeling and Analysis* pp. 60-64. Springer, New York.
- Knudson M. D., Hanson D. L., Bailey J. E., Hall C. A., Asay J.R., et al. (2004) *Phys. Rev. B*, 69, 144209.
- Knutson H., Charbonneau D., Noyes R. W., Brown T. M., and Gilliland R. L. (2006) *Astrophys. J.*, submitted.
- Konacki M., Torres G., Jha S., and Sasselov D. D. (2003a) *Nature*, 421, 507-509.
- Konacki M., Torres G., Sasselov D. D., and Jha S. (2003b) *Astrophys. J.*, 597, 1076-1091.
- Konacki M., Torres G., Sasselov D. D., Pietrzynski G., Udalski A., et al. (2004) *Astrophys. J.*, 609, L37-L40.
- Konacki M., Torres G., Sasselov D. D., and Jha S. (2005) *Astrophys. J.*, 624, 372-377.
- Kovács G., Zucker S., and Mazeh T. (2002), *Astron. Astrophys.*, 391, 369-377.
- Kurucz R. (1992) In *The Stellar Populations of Galaxies* (B. Barbuy and A. Renzini, eds.), pp. 225-232. Kluwer, Dordrecht.
- Latham D. W. (2003) In *Scientific Frontiers in Research on Extrasolar Planets* (D. Deming and S. Seager, eds.), pp. 409-412. ASP Conf. Series, San Francisco.
- Laughlin G., Wolf A., Vanmunster T., Bodenheimer P., Fischer D., et al. (2005a) *Astrophys. J.*, 621, 1072-1078.
- Laughlin G., Marcy G. W., Vogt, S. S., Fischer D. A., and Butler R. P. (2005b) *Astrophys. J.*, 629, L121-L124.
- Lecavelier des Etangs A., Vidal-Madjar A., McConnell J. C., and Hébrard G. (2004) *Astron. Astrophys.*, 418, L1-L4.
- Leigh C., Collier Cameron A., Udry S., Donati J.-F., Horne K., et al. (2003a) *Mon. Not. R. Astron. Soc.*, 346, L16-L20.
- Leigh C., Collier Cameron A., Horne K., Penny A., and James D. (2003b) *Mon. Not. R. Astron. Soc.*, 344, 1271-1282.
- Lin D. N. C., Bodenheimer P., and Richardson D. C. (1996) *Nature*, 380, 606-607.
- Lindal G. F., Wood G. E., Levy G. S., Anderson J. D., Sweetnam D. N., et al. (1981) *J. Geophys. Res.*, 86, 8721-8727.
- Lissauer J. J. (1993) *Ann. Rev. Astron. Astrophys.*, 31, 129-174.
- Mallen-Ornelas G., Seager S., Yee H. K. C., Minniti D., Gladders M. D. et al. (2003) *Astrophys. J.*, 582, 1123-1140.
- Mandel K. and Agol E. (2002) *Astrophys. J.*, 580, L171-L174.
- Mandushev G., Torres G., Latham D. W., Charbonneau D., Alonso R., et al. (2005) *Astrophys. J.*, 621, 1061-1071.
- Marley M. S., Gelino C., Stephens D., Lunine J. I., and Freedman R. (1999) *Astrophys. J.*, 513, 879-893.
- Marshall J. L., Burke C. J., DePoy D. L., Gould A., and Kollmeier

- J. A. (2005) *Astron. J.*, 130, 1916-1928.
- Mayor M. and Queloz D. (1995) *Nature*, 378, 355-359.
- Mazeh T., Naef D., Torres G., Latham D. W., Mayor M., et al. (2000) *Astrophys. J.*, 532, L55-L58.
- McArthur B. E., Endl M., Cochran W. D., Benedict G. F., Fischer D. A., et al. (2004) *Astrophys. J.* 614, L81-L84.
- McCullough P. R., Stys J. E., Valenti J. A., Fleming S. W., Janes K. A., et al. (2005) *Publ. Astron. Soc. Pac.*, 117, 783-795.
- McLaughlin D. B. (1924) *Astrophys. J.*, 60, 22-31.
- Menou K., Cho J. Y-K., Hansen B. M. S., and Seager S. (2003) *Astrophys. J.*, 587, L113-L116.
- Militzer B. and Ceperley D. M. (2001) *Phys. Rev. E*, 63, 066404.
- Miralda-Escudé J. (2002) *Astrophys. J.*, 564, 1019-1023.
- Mizuno H. (1980) *Prog. Theor. Phys.*, 64, 544-557.
- Mochejska B. J., Stanek K. Z., Sasselov D. D., Szentgyorgyi A. H., Bakos G. Á., et al. (2005) *Astron. J.*, 129, 2856-2868.
- Mochejska B. J., Stanek K. Z., Sasselov D. D., Szentgyorgyi A. H., Adams E. et al. (2006) *Astron. J.*, 131, 1090-1105.
- Moutou C., Coustenis A., Schneider J., St Gilles R., Mayor M., et al. (2001) *Astron. Astrophys.*, 371, 260-266.
- Moutou C., Coustenis A., Schneider J., Queloz D., and Mayor M. (2003) *Astron. Astrophys.*, 405, 341-348.
- Moutou C., Pont F., Bouchy F., and Mayor M. (2004) *Astron. Astrophys.*, 424, L31-L34.
- Murray N., Hansen B., Holman M., and Tremaine S. (1998), *Science*, 279, 69-72.
- Narita N., Suto Y., Winn J. N., Turner E. L., Aoki W., et al. (2005) *Publ. Astron. Soc. Japan*, 57, 471-480.
- O'Donovan, F. T., Charbonneau D., Torres G., Mandushev G., Dunham E. W., et al. (2006) *Astrophys. J.*, in press.
- Ohta Y., Taruya A., and Suto Y. (2005) *Astrophys. J.*, 622, 1118-1135.
- Peale S. J. (1969) *Astron. J.*, 74, 483-489.
- Pepper J. and Gaudi B. S. (2005) *Astrophys. J.*, 631, 581-596.
- Pepper J. and Gaudi B. S. (2006) *Acta Astron.*, submitted.
- Pepper J., Gould A., and Depoy, D. L. (2003) *Acta Astron.*, 53, 213-228.
- Pepper J., Gould A., and Depoy D. L. (2004) In *The Search for Other Worlds* (S. Holt and D. Deming, eds.), pp. 185-188. AIP Conf. Series.
- Pollack J. B. Hubickij O., Bodenheimer P., Lissauer J. J., Podolak M., et al. (1996) *Icarus*, 124 62-85.
- Pont F., Bouchy F., Queloz D., Santos N. C., Melo C., et al. (2004) *Astron. Astrophys.*, 426, L15-L18.
- Pont F., Bouchy F., Melo C., Santos N.C., Mayor M., et al. (2005) *Astron. Astrophys.*, 438, 1123-1140.
- Queloz D., Eggenberger A., Mayor M., Perrier C., Beuzit J. L., et al. (2000) *Astron. Astrophys.*, 359, L13-L17.
- Rauer H., Eislöffel J., Erikson A., Guenther E., Hatzes A. P., et al. (2004) *Publ. Astron. Soc. Pac.*, 116, 38-45.
- Richardson L. J., Deming D., and Seager S. (2003a) *Astrophys. J.*, 597, 581-589.
- Richardson L. J., Deming D., Wiedemann G., Goukenleuque C., Steyert D., et al. (2003b) *Astrophys. J.*, 584, 1053-1062.
- Rivera E. J., Lissauer J. J., Butler R. P., Marcy G. W., Vogt S. S., et al. (2005) *Astrophys. J.*, 634, 625-640.
- Rossiter R. A. (1924) *Astrophys. J.*, 60, 15-21.
- Santos N. C., Bouchy F., Mayor M., Pepe F., Queloz D., et al. (2004) *Astron. Astrophys.*, 426, L19-L23.
- Sato B., Fischer D. A., Henry G. W., Laughlin G., Butler R. P., et al. (2005) *Astrophys. J.*, 633, 465-473.
- Saumon D. and Guillot T. (2004) *Astrophys. J.*, 460, 993-1018.
- Saumon D., Chabrier G., Wagner D. J., and Xie X. (2000) *High Press. Res.*, 16, 331-343.
- Seager S. and Mallen-Ornelas G. (2003) *Astrophys. J.*, 585, 1038-1055.
- Seager S. and Sasselov D. D. (1998) *Astrophys. J.*, 502, L157-L161.
- Seager S. and Sasselov D. D. (2000) *Astrophys. J.*, 537, 916-921.
- Seager S., Whitney B. A., and Sasselov D. D. (2000) *Astrophys. J.*, 540, 504-520.
- Seager S., Richardson L. J., Hansen B. M. S., Menou K., Cho J. Y-K., et al. (2005) *Astrophys. J.*, 632, 1122-1131.
- Showman A. P. and Guillot T. (2002) *Astron. Astrophys.*, 385, 166-180.
- Silva A. V. R. (2003) *Astrophys. J.*, 585, L147-L150.
- Sirko E. and Paczyński B. (2003) *Astrophys. J.*, 592, 1217-1224.
- Sozzetti A., Yong D., Torres G., Charbonneau D., Latham D. W., et al. (2004) *Astrophys. J.*, 616, L167-L170.
- Steffen J. H. and Agol E. (2005), *Mon. Not. R. Astron. Soc.* 364, L96-L100.
- Struve O. (1952) *Observatory*, 72, 199-200.
- Sudarsky D., Burrows A., and Pinto P. (2000) *Astrophys. J.*, 538, 885-903.
- Sudarsky D., Burrows A., and Hubeny I. (2003) *Astrophys. J.*, 588, 1121-1148.
- Tingley B. (2004) *Astron. Astrophys.*, 425, 1125-1131.
- Torres G., Konacki M., Sasselov D. D., and Jha S. (2004a), *Astrophys. J.*, 609, 1071-1075.
- Torres G., Konacki M., Sasselov D. D., and Jha S. (2004b), *Astrophys. J.*, 614, 979-989.
- Torres G., Konacki M., Sasselov D. D., and Jha S. (2005), *Astrophys. J.*, 619, 558-569.
- Udalski A., Paczynski B., Zebrun K., Szymanski M., Kubiak M., et al. (2002a) *Acta Astron.*, 52, 1-37.
- Udalski A., Zebrun K., Szymanski M., Kubiak M., Soszynski I., et al. (2002b) *Acta Astron.*, 52, 115-128.
- Udalski A., Szewczyk O., Zebrun K., Pietrzynski G., Szymanski M., et al. (2002c) *Acta Astron.*, 52, 317-359.
- Udalski A., Pietrzynski G., Szymanski M., Kubiak M., Zebrun K., et al. (2003) *Acta Astron.*, 53, 133-149.
- Udalski A. Szymanski M. K., Kubiak M., Pietrzynski G., Soszynski I., et al. (2004) *Acta Astron.*, 54, 313-345.
- Vidal-Madjar A., Lecavelier des Etangs A., Désert J.-M., Ballester G. E., Ferlet R., et al. (2003) *Nature*, 422, 143-146.
- Vidal-Madjar A., Désert J.-M., Lecavelier des Etangs A., Hébrard G., Ballester G. E., et al. (2004) *Astrophys. J.*, 604, L69-L72.
- von Braun K., Lee B. L., Seager S., Yee H. K. C., Mallén-Ornelas G., et al. (2005) *Publ. Astron. Soc. Pac.*, 117, 141-159.
- Walker G., Matthews J., Kuschnig R., Johnson R., Rucinski S., et al. (2003) *Publ. Astron. Soc. Pac.*, 115, 1023-1035.
- Williams P. K. G., Charbonneau D., Cooper C. S., Showman A. P., and Fortney J. J. (2006) *Astrophys. J.*, submitted.
- Winn J. and Holman M. J. (2005) *Astrophys. J.*, 628, L159-L162.
- Winn J. N., Suto Y., Turner E. L., Narita N., Frye B. L., et al. (2004) *Publ. Astron. Soc. Japan*, 56, 655-662.
- Winn J. N., Noyes R. W., Holman M. J., Charbonneau D., Ohta Y., et al. (2005) *Astrophys. J.*, 631, 1215-1226.
- Wittenmyer R. A., Welsh W. F., Orosz J. A., Schultz A. B., Kinzel W., et al. (2005) *Astrophys. J.*, 632, 1157-1167.
- Wolf A., Laughlin G., Henry G. W., Fischer D. A., Marcy G., et al. (2006) *Astrophys. J.*, in press.